Parametric Images of Myocardial Viability Using a Single ^{15}O-H_2O PET/CT Scan

Hendrik J. Harms[1], Stefan de Haan[2], Paul Knaapen[2], Cornelis P. Allaart[2], Adriaan A. Lammertsma[1], and Mark Lubberink[1]

[1]*Department of Nuclear Medicine and PET Research, VU University Medical Center, Amsterdam, The Netherlands; and* [2]*Department of Cardiology, VU University Medical Center, Amsterdam, The Netherlands*

Perfusable tissue index (PTI) is a marker of myocardial viability and requires acquisition of transmission, ^{15}O-CO, and ^{15}O-H_2O scans. The aim of this study was to generate parametric PTI images from a ^{15}O-H_2O PET/CT scan without an additional ^{15}O-CO scan. **Methods:** Data from 20 patients undergoing both ^{15}O-H_2O and ^{15}O-CO scans were used, assessing correlation between PTI based on ^{15}O-CO (PTI_{CO}) and on fitted blood volume fractions (PTI_{Vb}). In addition, parametric PTI_{Vb} images of 10 patients undergoing ^{15}O-H_2O PET/CT scans were generated using basis-function methods and compared with PTI_{Vb} obtained using nonlinear regression. Simulations were performed to study the effects of noise on PTI_{Vb}. **Results:** Correlation between PTI_{CO} and PTI_{Vb} was high ($r^2 = 0.73$). Parametric PTI_{Vb} correlated well with PTI_{Vb} obtained using nonlinear regression ($r^2 = 0.91$). Simulations showed low sensitivity to noise (coefficient of variation $< 10\%$ at 20% noise). **Conclusion:** Parametric PTI images can be generated from a single ^{15}O-H_2O PET/CT scan.

Key Words: myocardial viability; PET/CT; parametric images

J Nucl Med 2011; 52:745–749
DOI: 10.2967/jnumed.110.085431

Detection of viable myocardium in patients with coronary artery disease is of great clinical importance. In contrast to nonviable myocardium, viable hibernating myocardium is capable of regaining contractility after revascularization, leading to improved cardiac function and associated patient prognosis (*1*).

PET using ^{15}O-H_2O (*2,3*) is considered to be the gold standard for measuring myocardial blood flow (MBF). In addition, the combination of ^{15}O-H_2O MBF and ^{15}O-CO blood volume scans enables the calculation of perfusable tissue index (PTI), a validated marker of myocardial viability (*4–10*). PTI is defined as the ratio of water perfusable and anatomic tissue fractions (PTFs and ATFs, respectively). PTF is, together with MBF, obtained from a ^{15}O-H_2O scan, whereas ATF is calculated by subtracting a normalized ^{15}O-CO blood-pool image from a transmission image. The ^{15}O-CO scan has no clinical use other than measuring blood volume. It prolongs overall study duration and thereby increases risk of patient motion during a study. On stand-alone PET scanners, acquisition of transmission scans using ^{68}Ge sources takes about 10 min, further prolonging study duration. Furthermore, for these scanners it was not possible to generate parametric MBF or PTF images of reasonable quality (*11*), ruling out parametric PTI images as well. These factors have limited the use of PTI in routine clinical practice.

Introduction of hybrid PET/CT scanners in cardiac PET (*12,13*), using low-dose (LD) CT for attenuation correction, reduces overall scan time and thus risk of patient motion between emission and transmission scans. Furthermore, improvements in detector efficiency and implementation of basis-function methods (BFM) (*11,14*) have enabled accurate calculation of MBF at a voxel level, resulting in parametric MBF images of diagnostic quality (*15*). When calculating MBF images, additional images of PTF, arterial and right-ventricular blood volume (V_A and V_{RV} (*16*), respectively), and spillover fractions are also obtained. Because all these images are calculated from the same dynamic scan, by definition, they do not suffer from interscan patient motion. Consequently, using blood volume fraction images and fast LD CT scans should enable generation of parametric PTI images of diagnostic quality.

The aim of this study was to develop and validate a method for generation of parametric PTI images based on a ^{15}O-H_2O PET/CT scan without an additional ^{15}O-CO blood-pool scan.

MATERIALS AND METHODS

Patient Data

Existing data from 20 patients (mean age, 61 y; age range, 34–83 y; 13 men, 7 women) with known or suspected ischemic cardiomyopathy, who had undergone both ^{15}O-H_2O and ^{15}O-CO scans on a stand-alone PET scanner, were used. In addition, 10 patients (mean age, 66 y; age range, 55–80 y; 5 men, 5 women) with ischemic cardiomyopathy (ejection fraction $< 35\%$) underwent ^{15}O-H_2O PET/CT scans. The study was approved by the

Received Nov. 18, 2010; revision accepted Jan. 31, 2011.
For correspondence or reprints contact: Hendrik J. Harms, Department of Nuclear Medicine and PET Research, VU University Medical Center, P.O. Box 7057, 1007 MB Amsterdam, The Netherlands.
E-mail: h.harms@vumc.nl

institutional Medical Ethics Review Committee, and all participants gave written informed consent.

Image Acquisition

Stand-Alone PET. Both ^{15}O-CO and ^{15}O-H_2O scans were obtained in 2-dimensional acquisition mode using an ECAT EXACT HR+ scanner (Siemens/CTI) according to a protocol that has been described previously (*9*).

PET/CT. ^{15}O-H_2O scans were acquired using a Gemini TF-64 PET/CT scanner (Philips Healthcare). ^{15}O-H_2O (370 MBq) was administered intravenously, simultaneously starting with a 6-min list-mode emission scan. This PET scan was followed immediately by a slow non–cardiac or respiration-gated LD CT scan (*17*) to ensure that conditions for this scan were comparable to those for the transmission scan of the stand-alone PET studies. Images were reconstructed into 22 frames of increasing duration, as described previously (*17*).

Validation of PTI Based on Fitted Blood Volume Fractions (PTI_{Vb})

Arterial and venous time–activity curves ($C_A(t)$ and $C_{RV}(t)$, respectively) were obtained as described previously (*17*). Traditional ATF ($g \cdot mL^{-1}$) images were constructed as described elsewhere (*9*); these were rotated to obtain short-axis images of the heart. Sixteen myocardial-segment volumes of interest were drawn manually on ATF images according to the 17-segment model of the American Heart Association, excluding the apex. This volume-of-interest template was projected onto both short-axis transmission and emission scans. Segment time–activity curves were extracted, and MBF ($mL \cdot g^{-1} \cdot min^{-1}$), PTF ($g \cdot mL^{-1}$), and V_A and V_{RV} (both dimensionless) were obtained using nonlinear regression (NLR) of the single-tissue-compartment model, with corrections for spillover and partial-volume effects (*3,16*):

$$C_T(t) = PTF \times MBF \times C_A(t) \otimes e^{-\frac{MBF}{V_T} \times t} + V_A \times C_A(t) + V_{RV} \times C_{RV}(t), \quad \text{Eq. 1}$$

where V_A represents arterial blood volume and left-ventricular spillover fraction, V_{RV} right-ventricular spillover fraction, and V_T the partition coefficient of water (which was fixed to 0.91 $mL \cdot g^{-1}$). Finally, PTI based on ^{15}O-CO (PTI_{CO}) and PTI_{Vb} was calculated using

$$PTI_{CO} = \frac{PTF}{ATF} = \frac{PTF}{1.06 \times (Tx_{norm} - CO)}, \quad \text{Eq. 2}$$

$$PTI_{Vb} = \frac{PTF}{1.06 \times (Tx_{norm} - V_A - V_{RV})}, \quad \text{Eq. 3}$$

in which Tx_{norm} (dimensionless) is the normalized transmission scan (*9*), CO is the normalized ^{15}O-CO concentration, and 1.06 represents the density of blood. Correlation and agreement of PTI_{Vb} and PTI_{CO} were assessed using both linear regression with zero intercept and Bland–Altman analysis.

Parametric PET/CT Images

Parametric images were generated using a BFM implementation (*11,14,15*) of Equation 1, as described previously (*17*). Attenuation-correction images based on the LD CT scan were normalized, and parametric images of V_A and V_{RV} were subtracted to obtain parametric ATF_{Vb} (ATFs based on fitted blood volume fractions) images. PTI_{Vb} images were then calculated as the ratio of PTF and ATF_{Vb} images. ATF and PTF of voxels with a total blood volume fraction above 0.75, an ATF below 0.25, or a PTF below 0.1 were set to 0 to avoid noise-induced high PTI levels in blood vessels or outside the heart. Average segmental PTI_{Vb} was compared with PTI_{Vb} calculated from segmental time–activity curves using linear regression with zero intercept, intraclass correlation coefficient (ICC), and Bland–Altman analysis.

Simulations

Simulations were performed for both BFM and NLR using $C_A(t)$ and $C_{RV}(t)$ of a randomly selected patient imaged on the PET/CT scanner. Tissue time–activity curves $C_{tissue}(t)$ were generated for MBF of 1 $mL \cdot g^{-1} \cdot min^{-1}$ and PTI_{Vb} levels of 0.5 and 1.0, which represent (nontransmural) scar and healthy tissue, respectively. Tx_{norm} was fixed to 1 and considered to be noise-free. Different levels of gaussian noise were added to $C_{tissue}(t)$ (4% and 20%), representing segmental and voxel noise levels, respectively. Lower noise (1%) was added to $C_A(t)$ and $C_{RV}(t)$, as these time–activity curves are based on large volumes of interest.

Next, MBF, V_A, V_{RV}, and PTF were obtained using both NLR and BFM. This process was repeated 1,000 times for each combination of noise on $C_A(t)$, $C_{RV}(t)$, and $C_{tissue}(t)$. Average PTI_{Vb} values, together with corresponding bias and coefficient of variation (COV), were calculated for each combination of noise level and PTI_{Vb}.

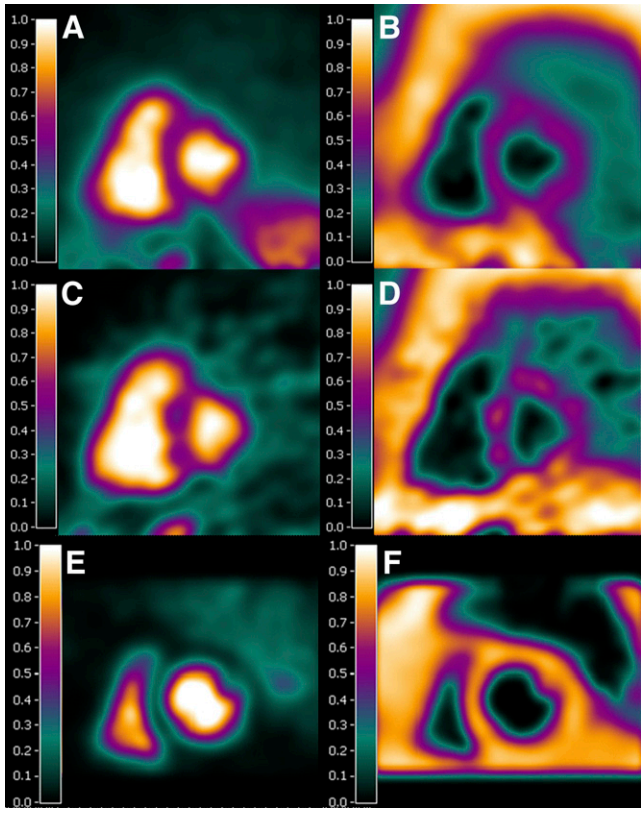

FIGURE 1. Example of short-axis fractional blood volume (A and C) and ATF (B and D) images obtained from ^{15}O-CO (A and B) and fitted blood volume fraction (C and D) images of same patient. Images were obtained using stand-alone PET scanner and 10-mm gaussian filter. Also shown is example of short-axis fractional blood volume (E) and ATF (F) images obtained using clinical PET/CT scanner and fitted blood volume fraction images.

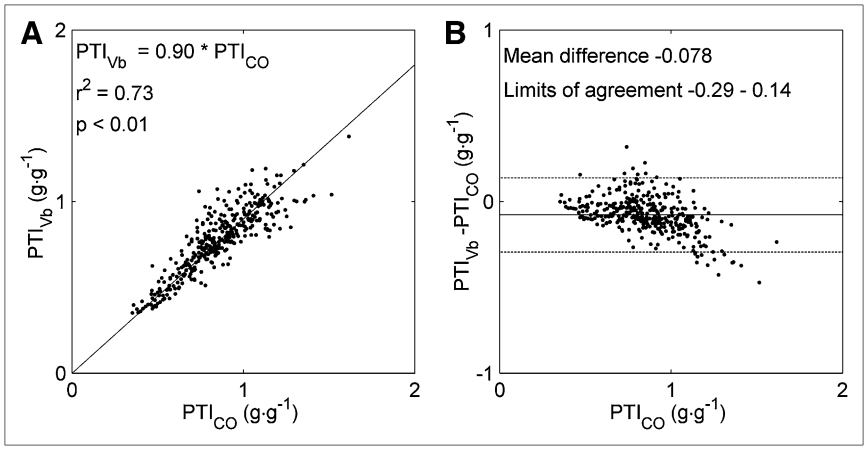

FIGURE 2. Correlation between segmental PTI, obtained using stand-alone PET scanner, based on fitted ^{15}O-H_2O blood volume fraction and ^{15}O-CO blood volume images (A) with corresponding Bland–Altman plot (B).

RESULTS

Validation of PTI_{Vb}

Figures 1A and 1B show short-axis blood volume and ATF images, respectively, obtained from a ^{15}O-CO scan acquired on the stand-alone PET scanner. For the same patient and scanner, corresponding images based on fitted blood volume fraction images are shown in Figures 1C and 1D. Finally, blood volume and ATF images based on fitted blood volume fraction images for another patient acquired on the PET/CT scanner are shown in Figures 1E and 1F, respectively. Figure 2 shows correlation and agreement between PTI_{CO} and PTI_{Vb}. Correlation and agreement were high ($r^2 = 0.73$; ICC = 0.86). The slope of the linear regression was 0.90, which was significantly different from 1 ($P < 0.001$).

Parametric PET/CT Images

A parametric PTI_{Vb} image of a typical patient with a known myocardial infarction can be seen in Figure 3. This patient also underwent delayed contrast-enhanced (DCE) MRI, and the corresponding DCE MR image is shown for illustration. Correlation and agreement of PTI_{Vb} obtained using NLR on segmental time–activity curves and directly from parametric images were high ($r^2 = 0.91$; ICC = 0.95), as shown in Figure 4. The slope of the linear regression between both parameters was not significantly different from 1 ($P > 0.05$).

Simulations

Results of the simulations are summarized in Table 1. Accuracy and precision of both NLR and BFM were high, with no significant bias and a COV less than 10%, even at high noise levels.

DISCUSSION

In the present study, a method for generating parametric PTI images from a single ^{15}O-H_2O PET/CT scan was developed and evaluated. This method makes use of fitted blood volume fractions derived from the ^{15}O-H_2O scan itself rather than using an (additional) ^{15}O-CO scan.

The slope of the linear fit between PTI_{CO} and PTI_{Vb} was 0.90 and significantly lower than 1. This may be due to the fact that the V_{RV} represents only spillover from the right ventricle but not the actual venous blood volume fraction (V_V) of the myocardium. Actual V_V in myocardial tissue is approximately 10% (*18*), and consequently ATF_{Vb} is 10% higher than ATF based on ^{15}O-CO, leading to values 10% lower for PTI_{Vb} than for PTI_{CO} (i.e., slope of linear fit, 0.90). This overestimation due to V_V is, however, also seen in PTF because the model used for kinetic analysis of ^{15}O-H_2O data cannot distinguish venous blood from tissue (concentrations are similar). In PTI_{CO}, V_V is included in PTF but not in ATF—possibly becoming a source of error during PTI_{CO} measurements because of the large spread of venous blood volumes (average V_V of 0.093 ± 0.103 $mL \cdot g^{-1}$) (*19*). Because V_V is included in both PTF and ATF_{Vb}, PTI_{Vb} should be less sensitive to changes in V_V.

Using a clinical PET/CT scanner, the proposed method resulted in parametric PTI images of diagnostic quality, enabling simultaneous imaging of myocardial viability and perfusion based solely on a 6-min ^{15}O-H_2O scan, followed by a short (<1 min) LD CT scan. The use of a fast LD CT instead of a (longer) transmission scan based on ^{68}Ge sources, as is common in stand-alone PET scanners, reduces the risk

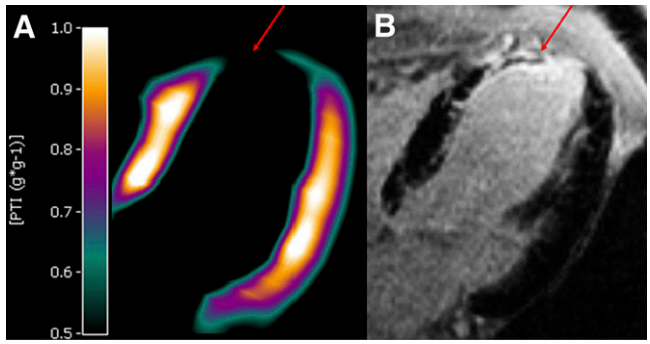

FIGURE 3. Parametric PTI_{Vb} image obtained using PET/CT scanner (A) and corresponding DCE MR image (B) of typical patient with myocardial infarction, indicated by reduced PTI_{Vb} and hyperenhancement in DCE MR image. Arrows indicate myocardial infarction.

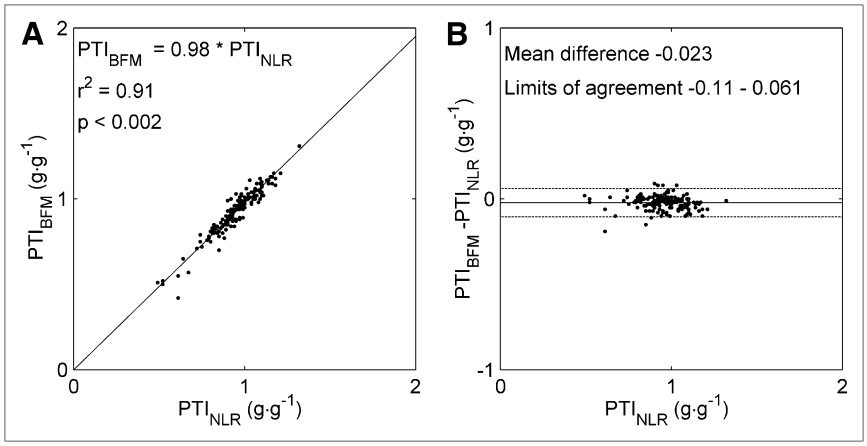

FIGURE 4. Correlation between average segmental PTI and PTI obtained using NLR (PTI_{NLR}) of segmental time–activity curves (A), with corresponding Bland–Altman plot (B) obtained using PET/CT scanner.

of patient motion between scans, improving reliability and image quality of parametric PTI_{Vb} images. Using a slow-respiration–averaged LD CT scan ensures that the transmission scans are obtained under the same conditions (i.e., normal breathing) as traditional transmission scans. Image quality was further improved by scanning in 3-dimensional mode, because noise-equivalent count rates in 3-dimensional mode are typically 3–5 times higher than rates in 2-dimensional mode. Even in 3-dimensional acquisition mode, however, the need for an additional ^{15}O-CO scan could still hamper accurate parametric images in some patients because of mismatch between scans. The method described here overcomes this issue.

Simulations showed that even at noise levels typically seen in voxel time–activity curves, PTI_{Vb} could be calculated with high accuracy and precision (COV, 10%, no significant bias). Furthermore, flow heterogeneity, a possible source of bias in PTI (*20*), is expected to be much smaller in individual voxels (4 × 4 × 4 mm), reducing possible bias when using parametric PTI images.

Thresholds used for generating parametric images were chosen empirically, based on previous results (*17*). Further studies are needed to optimize these thresholds. Furthermore, it could be of interest to directly compare parametric PTI_{Vb} and PTI_{CO} images on a clinical PET/CT scanner.

TABLE 1
COV (%) and Relative Bias (%) Derived from Simulations (n = 1,000 for Each Condition) of Scar and Healthy (PTI = 0.5 and 1.0, Respectively) Tissue

	Scar		Healthy	
Method	ROI	Voxel	ROI	Voxel
NLR				
COV	1.44	7.05	1.60	8.82
Bias	−0.04	−0.82	−0.10	−0.33
BFM				
COV	2.16	10.43	1.77	8.88
Bias	0.09	1.14	−0.12	−0.36

ROI and voxel noise levels were 4% and 20%, respectively.

CONCLUSION

The proposed method enables calculation of parametric PTI_{Vb} images based solely on a single myocardial ^{15}O-H_2O scan and an LD CT scan. This method reduces scan duration, radiation dose, and risk of patient motion between scans and enables simultaneous and quantitative assessment of both myocardial perfusion and viability with a 10-min scanning protocol.

DISCLOSURE STATEMENT

The costs of publication of this article were defrayed in part by the payment of page charges. Therefore, and solely to indicate this fact, this article is hereby marked "advertisement" in accordance with 18 USC section 1734.

ACKNOWLEDGMENTS

We thank Suzette van Balen, Judith van Es, Amina Elouahmani, Femke Jongsma, Nazerah Sais, and Annemiek Stiekema for scanning patients; Dr. Gert Luurtsema, Robert Schuit, Kevin Takkenkamp, and Henri Greuter for production of ^{15}O-H_2O; and Dr. Marc Huisman for helpful comments on the manuscript. This work was supported financially by Philips Healthcare.

REFERENCES

1. Wijns W, Vatner SF, Camici PG. Hibernating myocardium. *N Engl J Med.* 1998;339:173–181.
2. Bergmann SR, Fox KA, Rand AL, et al. Quantification of regional myocardial blood flow in vivo with $H_2{}^{15}O$. *Circulation.* 1984;70:724–733.
3. Iida H, Kanno I, Takahashi A, et al. Measurement of absolute myocardial blood flow with $H_2{}^{15}O$ and dynamic positron-emission tomography: strategy for quantification in relation to the partial-volume effect. *Circulation.* 1988;78:104–115.
4. Yamamoto Y, De SR, Rhodes CG, et al. A new strategy for the assessment of viable myocardium and regional myocardial blood flow using ^{15}O-water and dynamic positron emission tomography. *Circulation.* 1992;86:167–178.
5. De Silva R, Yamamoto Y, Rhodes CG, et al. Preoperative prediction of the outcome of coronary revascularization using positron emission tomography. *Circulation.* 1992;86:1738–1742.
6. Iida H, Tamura Y, Kitamura K, Bloomfield PM, Eberl S, Ono Y. Histochemical correlates of ^{15}O-water-perfusable tissue fraction in experimental canine studies of old myocardial infarction. *J Nucl Med.* 2000;41:1737–1745.

7. Itoh H, Namura M, Seki H, et al. Perfusable tissue index obtained by positron emission tomography as a marker of myocardial viability in patients with ischemic ventricular dysfunction. *Circ J.* 2002;66:341–344.
8. Knaapen P, Boellaard R, Gotte MJ, et al. The perfusable tissue index: a marker of myocardial viability. *J Nucl Cardiol.* 2003;10:684–691.
9. Knaapen P, Boellaard R, Gotte MJ, et al. Perfusable tissue index as a potential marker of fibrosis in patients with idiopathic dilated cardiomyopathy. *J Nucl Med.* 2004;45:1299–1304.
10. Knaapen P, Bondarenko O, Beek AM, et al. Impact of scar on water-perfusable tissue index in chronic ischemic heart disease: evaluation with PET and contrast-enhanced MRI. *Mol Imaging Biol.* 2006;8:245–251.
11. Boellaard R, Knaapen P, Rijbroek A, Luurtsema GJ, Lammertsma AA. Evaluation of basis function and linear least squares methods for generating parametric blood flow images using ^{15}O-water and positron emission tomography. *Mol Imaging Biol.* 2005;7:273–285.
12. Di Carli MF, Hachamovitch R. New technology for noninvasive evaluation of coronary artery disease. *Circulation.* 2007;115:1464–1480.
13. Knaapen P, de Haan S, Hoekstra OS, et al. Cardiac PET-CT: advanced hybrid imaging for the detection of coronary artery disease. *Neth Heart J.* 2010; 18:90–98.
14. Watabe H, Jino H, Kawachi N, et al. Parametric imaging of myocardial blood flow with ^{15}O-water and PET using the basis function method. *J Nucl Med.* 2005;46:1219–1224.
15. Harms HJ, Knaapen P, de Haan S, Halbmeijer R, Lammertsma AA, Lubberink M. Automatic generation of absolute myocardial blood flow images using [^{15}O] H_2O and a clinical PET/CT scanner. *Eur J Nucl Med Mol Imaging.* 2011;38:930–939.
16. Hermansen F, Rosen SD, Fath-Ordoubadi F, et al. Measurement of myocardial blood flow with oxygen-15 labelled water: comparison of different administration protocols. *Eur J Nucl Med.* 1998;25:751–759.
17. Lubberink M, Harms HJ, Halbmeijer R, de Haan S, Knaapen P, Lammertsma AA. Low-dose quantitative myocardial blood flow imaging using ^{15}O-water and PET without attenuation correction. *J Nucl Med.* 2010;51:575–580.
18. Crystal GJ, Downey HF, Bashour FA. Small vessel and total coronary blood volume during intracoronary adenosine. *Am J Physiol.* 1981;241:H194–H201.
19. Iida H, Rhodes CG, Araujo LI, et al. Noninvasive quantification of regional myocardial metabolic rate for oxygen by use of 15O2 inhalation and positron emission tomography: theory, error analysis, and application in humans. *Circulation.* 1996;94:792–807.
20. Herrero P, Staudenherz A, Walsh JF, Gropler RJ, Bergmann SR. Heterogeneity of myocardial perfusion provides the physiological basis of perfusable tissue index. *J Nucl Med.* 1995;36:320–327.